J. Am. Chem. Soc. 1990, 112, 7218-7221

CH Bond Activation in CH_4 and *t*-BuO(ads) by Oxygen Chemisorbed on Ag(110). Molecular Orbital Theory

Jenwei Yu and Alfred B. Anderson*

Contribution from the Chemistry Department, Case Western Reserve University, Cleveland, Ohio 44106. *Received March 5, 1990*

Abstract: Activation of the CH bond in CH_4 and *t*-BuO(ads) by H$^\bullet$ transfer to O adsorbed on the Ag(110) surface has been studied by the atom-superposition and electron-delocalization molecular orbital theory. Both abstractions are found to proceed with a low-energy barrier because of the presence of low-lying empty Ag surface orbitals at the Fermi level. Transfer of an electron to the Fermi level alleviates the initial closed-shell repulsion between the CH σ-bond electron pair and the surface O (which is formally O^{2-}) lone-pair orbital that ultimately forms the OH σ bond. It is concluded that surface O behaves like a radical anion $O^{\bullet-}$ or $R_3C^\bullet$ in its ability to form a single bond. This explains the experimental results of Brainard and Madix who observed the formation of isobutylene and isobutylene oxide from *t*-BuO(ads). Our calculations also suggest the possibility that surface oxygen atoms might insert into CH bonds to form alcohols, which is a result of their ability to exhibit O atom or carbene (R_2C:) bonding properties.

Silver is an important catalyst for oxidizing methanol to formaldehyde.[1] The kinetics and mechanisms have been studied by Wachs and Madix,[2] who found that surface oxygen atoms activate the dissociative methanol adsorption at 180 K to form CH_3O(ads) and H_2O(ads). The surface methoxide decomposes at 250–340 K by H transfer to Ag, forming H_2CO, some of which desorbs, and some of which reacts with CH_3O(ads), yielding methyl formate. Madix and co-workers have made similar studies of the activation of ethylene glycol[3,4] and *tert*-butyl alcohol[5] over oxygen-covered Ag(110) surfaces. Ethylene glycol loses both hydroxyl hydrogen atoms, yielding $-OCH_2CH_2O-$(ads), which is stable up to 350 K at which point re-forming and CH activation to glyoxal commences. *tert*-Butyl alcohol adsorbs dissociatively, forming $(CH_3)_3CO$(ads), which at 400 K begins to form isobutylene oxide and a lesser amount of isobutylene. In this reaction, a methyl hydrogen is transferred to a surface oxygen atom and the maximum thermal desorption rate occurs at 440 K. An additional and greater amount of products and some *tert*-butyl alcohol then begin to desorb with a peak at 510 K. The simultaneous appearance of the alcohol with reaction products during the higher temperature desorption led Brainard and Madix to suggest that methyl hydrogen from one adsorbed *tert*-butoxide anion is transferred to oxygen in a neighboring one.

It has been known from many experimental studies[6-9] that on oxide surfaces O^- species can abstract H$^\bullet$ from methane. Theoretical studies from our group involving O^- on MoO_3,[10] $CuMoO_4$,[11] and MgO[12] have found that the key feature in these abstraction reactions is that the surface O^- provides a low-lying half-filled orbital that takes one electron from the CH–O σ^*-antibonding orbital during the process of CH bond breaking and OH bond formation. The reaction is

$$CH_4(g) + O^-(s) \rightarrow CH_3^\bullet(g) + OH^-(s) \qquad (1)$$

Nondefective oxides, where only O^{2-} is on the surface, are less active in abstracting H because to form the products of reaction 1 an electron is also generated.

$$CH_4(g) + O^{2-}(s) \rightarrow CH_3(g) + OH^-(s) + e^- \qquad (2)$$

This electron must be promoted to the lowest available orbital, which in the oxide is the high-lying cation conduction band. On the above oxides this promotion energy prevents the reaction in eq 2. Bi_2O_3 is interesting because H$^\bullet$ abstraction can occur over it at temperatures elevated compared to the reaction in eq 1. A theoretical analysis[13] has attributed this activity to low-lying dangling surface Bi orbitals with energies in the O 2p–Bi valence bandgap. Because they are low-lying, they are relatively easily reduced so that the reaction in eq 2 becomes possible.

The initial interaction between a CH σ bond pair of electrons and an O^{2-} lone pair is a four-electron closed-shell repulsion. Low-lying empty (as is the case of Bi_2O_3) and half-filled (as in the case of O^-) orbitals remove an electron early in the interaction when CH collides with an oxygen anion. This activates the CH bond breaking, allowing the formation of $CH_3^\bullet$(g) and OH(s).

Oxygen atoms chemisorbed on Ag(110) in the work of the Madix group are formally oxide anions, O^{2-}, yet they are evidently abstracting H from *t*-BuO. From the above discussion it might be expected that low-lying orbitals are available for reduction and that they are likely to be the Ag conduction-band orbitals at the Fermi energy. In the present theoretical study, this idea is substantiated. Evidence for this effect giving adsorbed O-like and carbene-like (R_2C:) reactivities is also given.

Theory

The atom-superposition and electron-delocalization molecular orbital (ASED–MO) theory[14,15] is used. This is the method employed in the previous CH activation studies of refs 10–13. In it the Born–Oppenheimer energy, $E(R)$, of a molecular system is evaluated in two parts

$$E(R) = E_R(R) + E_D(R) \qquad (3)$$

where $E_R(R)$ is a repulsive pairwise atom superposition energy, $E_D(R)$ is an attractive energy caused by the electron charge density delocalization due to the bond formation, and R stands for the nuclear coordinates. $E_R(R)$ is determined by integrating the force on one of the nuclei as each pair of atoms (ab) is brought together

$$E_R(R) = \sum_{a<b} E_R^{ab}(R_{ab}) \qquad (4)$$

$$E_R^{ab}(R_{ab}) = Z_a\left(Z_b|R_a - R_b|^{-1} - \int \rho_a(r)\,|R_b - r|^{-1}\,dr\right) \qquad (5)$$

where Z are the nuclear charges and ρ are the atom density functions. $E_D(R)$ could be calculated in a similar sequence of steps

---

[1] Walker, J. F. *Formaldehyde*; Reinhold: New York, 1964.

[2] Wachs, I. E.; Madix, R. J. *Surf. Sci.* **1978**, *76*, 531.

[3] Capote, A. J.; Madix, R. J. *J. Am. Chem. Soc.* **1989**, *111*, 3570.

[4] Capote, A. J.; Madix, R. J. *Surf. Sci.* **1989**, *214*, 276.

[5] Brainard, R. L.; Madix, R. J. *J. Am. Chem. Soc.* **1989**, *111*, 3826.

[6] Kaliaguine, S. L.; Shelimov, B. N.; Kazansky, V. B. *J. Catal.* **1978**, *55*, 384.

[7] Ito, T.; Wang, J.-X.; Lin, C.-H.; Lunsford, J. H. *J. Am. Chem. Soc.* **1985**, *107*, 5062.

[8] Driscoll, D. J.; Martir, W.; Wang, J.-X.; Lunsford, J. H. *J. Am. Chem. Soc.* **1985**, *107*, 58.

[9] Driscoll, D. J.; Lunsford, J. H. *J. Phys. Chem.* **1985**, *89*, 4415.

[10] Mehandru, S. P.; Anderson, A. B.; Brazdil, J. F.; Grasselli, R. K. *J. Phys. Chem.* **1987**, *91*, 2930.

[11] Ward, M. D.; Brazdil, J. F.; Mehandru, S. P.; Anderson, A. B. *J. Phys. Chem.* **1987**, *91*, 6515.

[12] Mehandru, S. P.; Anderson, A. B.; Brazdil, J. F. *J. Am. Chem. Soc.* **1988**, *110*, 1715.

[13] Mehandru, S. P.; Anderson, A. B.; Brazdil, J. F. *J. Chem. Soc., Faraday Trans. 1* **1987**, *83*, 463.

[14] Anderson, A. B. *J. Chem. Phys.* **1975**, *62*, 1187.

[15] Anderson, A. B.; Grimes, R. W.; Hong, S. Y. *J. Phys. Chem.* **1987**, *91*, 4245.

0002-7863/90/1512-7218$02.50/0

Table I. Parameters Used in the Calculations[a]

	s			p			d					
atom	n	IP	ζ	n	IP	ζ	n	IP	ζ_1	ζ_2	c_1	c_2
H	1	12.10	1.200									
C	2	15.09	1.658	2	9.76	1.618						
O	2	26.98	2.146	2	12.12	2.127						
Ag	5	10.58	2.044	5	6.92	1.744	4	14.00	6.070	2.363	0.5780	0.6252

[a] Key: principal quantum number, n; orbital ionization potential, IP (eV); Slater orbital exponents, ζ (au); corresponding linear coefficients, c.

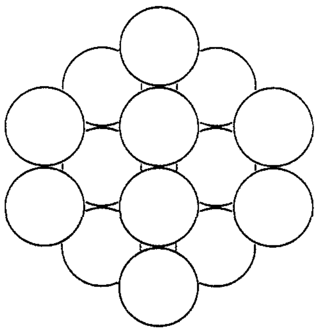

Figure 1. Ag_{14} cluster model of the (110) surface.

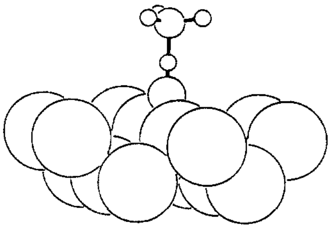

Figure 2. Transition state for H abstraction from CH_4 by a chemisorbed O atom.

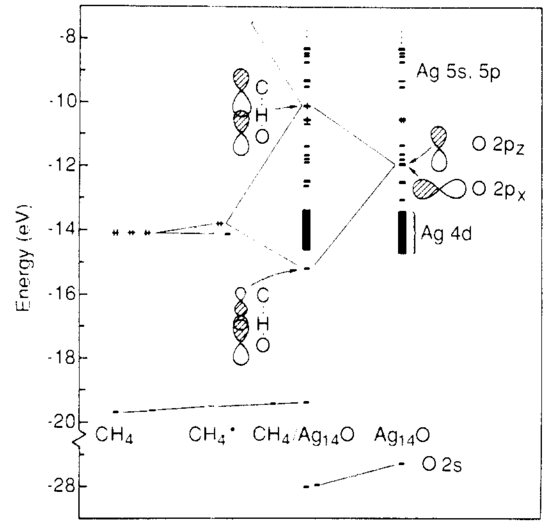

Figure 3. Orbital interactions at the transition state for H abstraction from CH_4 by a surface O as shown in Figure 2. The second column of levels is for CH_4 in the transition-state structure but not interacting with the $Ag_{14}O$ cluster.

were the electron delocalization density functions available, but they are not, so $E_D(R)$ must be approximated. A successful approximation is the following

$$E_D(R) \cong \Delta E_{MO}(R) = \sum_i n_i \epsilon_i^{MO}(R) - \sum_i n_i \epsilon_i^{a} \qquad (6)$$

where $\epsilon^{MO}(R)$ is the molecular orbital (delocalization) energy calculated by a Hamiltonian similar to extended Hückel, ϵ^a is an atomic orbital energy, n_i are orbital occupation numbers, and the summations are over molecular and atomic orbitals. When this approximation is used, each pairwise term of eq 5 is calculated according to the condition that atom a is more electronegative than atom b.

The atomic parameters in the ASED-MO theory are valence-state ionization potentials and Slater-type orbital exponents. Adjustments are made to the literature values in order to produce diatomic bond distances comparable to experimental values and charge transfers in accordance with the difference of Pauling's electronegativity. Parameters determined in this way in an earlier study[16] for Ag and O are used in the present work, and the C and H ionization potentials are increased by 1.5 eV, just as for O. The parameters are given in Table I.

Model

Our model for the Ag(110) surface is the two-layer-thick Ag_{14} cluster shown in Figure 1. The adsorption site for atomic oxygen on this surface has been on the topic of low-energy electron diffraction (LEED)[17,18] structure and electron energy loss (ELS)[19] vibrational analysis. Although a structure with oxygen sitting in the grooves between the first-layer Ag rows was suggested, a recent electron-stimulated desorption ion angular distributions (ESDIAD) study[20] raised doubt about the exact oxygen adsorption site. For studying CH activation in CH_4, we have chosen a model with an O in a 2-fold bridging site on the center of the Ag_{14} model shown in Figure 1. The O height is chosen such that the AgO distance is equal to the sum of atomic radii, 2.07 Å. This AgO distance is also used for surfaces OH and *t*-BuO. For surface *t*-BuO dehydrogenation the Ag_{14} cluster is again used, with the *t*-BuO group in the center, and an adjacent O atom is on a site as described below. In all structure determinations, bond length and angle optimizations are to 0.01 Å and 1°, respectively. Methyl group CH bond lengths, calculated to be 1.21 Å, are overestimated by 0.1 Å. In *t*-BuOH, the calculated CC bond lengths of 1.74 Å are overestimated by about 0.20 Å and the calculated CO bond length of 1.43 Å approximately matches experiment. OH bond lengths are calculated to be 1.01 Å in CH_3OH and *t*-BuOH and 1.00 Å in OH(ads), overestimating experiment by about 0.05 Å.

CH_4 Activation

When a CH bond in CH_4 approaches the oxygen atom on our Ag(110) surface cluster model vertically, the transition state shown in Figure 2 is found with an activation barrier of 1.41 eV. The CH bond stretches 0.24 Å, the OH distance is 1.19 Å, and the CH_3 group becomes flatter with H_3CH angles decreasing from the tetrahedral value of 109.5 to 101.5°, which is an indication of the impending formation of a planar CH_3 radical. The MO correlation diagram for the transition state is shown in Figure 3. The lowest unoccupied Ag_{14} cluster molecular orbital has predominately Ag 5s character, lying in the s band just above the highest occupied orbital. At the transition state, a three-centered CHO σ-donation bond has formed and its antibonding counterpart has carried two electrons up to the position of the lowest unoccupied orbital, where it is assumed to leave one electron behind. This orbital evolves into the half-filled $CH_3^{\bullet}$ radical orbital. The H 1s contribution to this orbital at the transition state is very small because of CH σ^*-orbital mixing, which becomes important as a result of the CH stretch that stabilizes it, and it in turn mixes with and stabilizes the antibonding counterpart to the CHO σ-donation orbital. The Ag surface acts as an electron sink and eliminates the CH bond pair–O^{2-} lone-pair closed-shell repulsion

---

(16) Mehandru, S. P.; Anderson, A. B. *Surf. Sci.* **1989**, *216*, 105.

(17) Heiland, W.; Iberl, F.; Taglauer, E. *Surf. Sci.* **1975**, *53*, 383.

(18) Engelhardt, H. A.; Menzel, D. *Surf. Sci.* **1976**, *57*, 591.

(19) Backx, C.; De Groot, C. P. M.; Biloen, P. *Surf. Sci.* **1981**, *104*, 300.

(20) Bange, K.; Madey, T. E.; Sass, J. K. *Chem. Phys. Lett.* **1985**, *113*, 56.

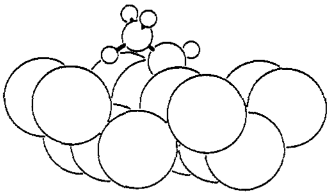

Figure 4. Calculated structure of adsorbed CH_3OH. The CO and HO distances and angles to the surface normal are 1.47 Å, 53° and 1.00 Å, 65°, respectively.

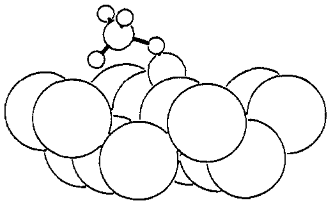

Figure 5. Calculated transition state for surface O inserting into a CH bond in CH_4.

at the transition state by allowing the antibonding counterpart to the filled CH σ-donation bonding orbital to lose an electron. Since the electron is transferred to the metal surface, the overall process is one of simultaneous proton transfer to O^{2-} and Ag reduction. This is evidenced by the charge on the adsorbed O atom that becomes 0.52 less negative at the CH_4 transition state to become −0.63. Because of the three-centered CHO σ delocalization, the CH_4 charge is +0.15. The overall reaction is

$$H_3C{:}H + {:}\ddot{\underset{..}{O}}{:}^{2-} \longrightarrow H_3C^{\bullet} + {:}\ddot{\underset{..}{O}}{:}H^{-} + e^{-}(cb) \qquad (7)$$

where the electron is promoted to the Ag conduction band.

The p orbitals with axes parallel to the plane of the surface, especially the p_x orbital with its axis along the (001) direction (from left to right in Figure 2), should be able to participate in the abstraction when the CH bond is tilted from the normal direction. As shown in Figure 3, the p_z (normal to the surface) and p_x (in the (001) direction) orbitals are nearly degenerate and so should readily hybridize to overlap with the CH σ orbital at such angles of approach. A nonnormal angle of approach is expected for dehydrogenation of adsorbed *t*-BuO. Therefore, we have examined the methane CH activation energy as a function of CH bond deviation from the surface normal while fixing all other structure parameters at the above-mentioned transition-state values and with tilting confined to the x–z plane. The activation energy is found to be unaffected to the first decimal place for deviation up to 50° from the surface normal, and at 60° deviation it increases by 0.07 eV. A minimum is found for a 40° tilt, which is 0.006 eV less than the activation energy obtained for the normal angle. This means the O p_x and p_z orbitals can effectively hybridize to maintain strong overlap with the CH σ orbital, activating the CH bond over a wide range of approach angles.

A gas-phase CH_3 radical is calculated to bind to the surface OH, as shown in Figure 4, with a stabilization energy of 2.55 eV. The reaction

$$CH_4(g) + O(ads) \rightarrow CH_3OH(ads) \qquad (8)$$

is calculated to be downhill by 1.00 eV on the Ag(110) surface. Thus, it would be interesting to know the barrier for this O insertion reaction. The calculated transition state is shown in Figure 5, and the barrier is 1.18 eV, which is 0.23 eV lower than for the H• abstraction reaction. The ease of promotion of two electrons to the Ag Fermi level is what gives the surface O^{2-} its carbene-like reactivity: two single bonds are easily formed during the insertion process. The oxenoid–carbenoid analogy has been noted by Tatsumi and Hoffmann,[21] and it is well-known that carbenes insert into single bonds. In the present transition state the CH bond stretches 0.24 Å, the OH distance is 1.10 Å, and the calculated Mulliken overlap population of the CO bond is 0.04 in the transition state, indicating that a CO bond is forming. Other parameters are a CO distance of 2.34 Å, with the CO axis 55° from the surface normal, and an OCH angle of 20°.

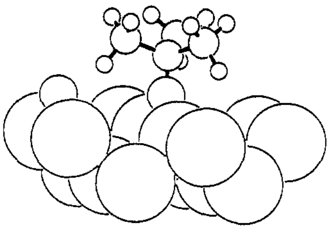

Figure 6. Structure of *t*-BuO(ads). Angles about all C are assumed to be tetrahedral, and the bond lengths are the calculated *t*-BuOH values.

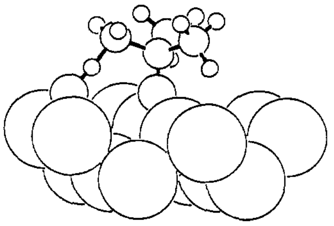

Figure 7. Calculated transition-state structure for H abstraction from *t*-BuO(ads) by a neighboring O(ads).

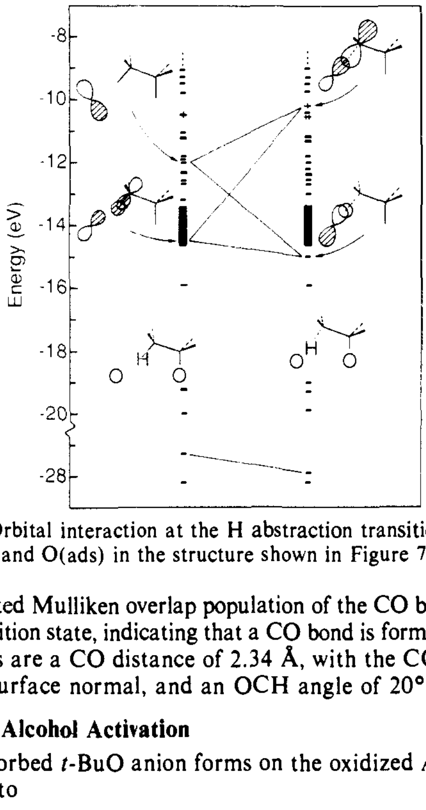

Figure 8. Orbital interaction at the H abstraction transition state for *t*-BuO(ads) and O(ads) in the structure shown in Figure 7.

tert-Butyl Alcohol Activation

The adsorbed *t*-BuO anion forms on the oxidized Ag surface according to

$$t\text{-BuOH} + O^{2-} \rightarrow t\text{-BuO}^{-} + OH^{-} \qquad (9)$$

Experimentally, the reaction proceeds at temperatures below 200 K to form *t*-BuO(ads) and H_2O, which desorbs. The electronic description of the OH activation should be the same as given above for CH activation, and the low temperature for alkoxide formation, which implies a low activation energy, in part reflects the stability of the reaction products.

Our model for studying methyl CH activation in *t*-BuO(ads) in the presence of adsorbed oxygen is shown in Figure 6. Only the structure parameters felt to be essential to the barrier are optimized. Theses are the CH stretch, the positions of O(ads) and *t*-BuO(ads) on the surface, and the H_2CH angles of the distorted CH_3 group. By moving O(ads) and *t*-BuO(ads) toward each other while keeping the AgO distance constant and optimizing the C–H stretch and the HCH angles, we obtain the transition state shown in Figure 7. The calculated barrier is 1.44 eV, essentially the same as calculated for CH_4 activation. The experimental Arrhenius activation energy is 0.9 eV.[5] The CH

---

[21] Tatsumi, K.; Hoffmann, R. *Inorg. Chem.* **1981**, *20*, 3771.

bond stretches 0.26 Å, the OH distance is 1.16 Å, and the H_2CH angles are 97.0° at the transition state, again similar to CH_4. The OHC angle is nearly 180°, and the tilt of the CH axis from the surface normal is nearly 40°. The O atoms each move 0.38 Å in the (001) direction. The MO correlation diagram is shown in Figure 8. Even before the CH bond is stretched, its proximity causes the surface p_z and p_x orbitals to hybridize: one hybrid is rotated to form the three-centered CHO donation bond and the other one is perpendicular to it and nonbonding with CH as shown in the left-hand column of Figure 8. Otherwise, the correlation diagram is essentially the same as for methane CH activation (Figure 3). At the transition state the antibonding counterpart to the σ-donation orbital has risen just past the Fermi level and has transferred an electron to the silver. By either desorbing as isobutylene or by forming isobutylene oxide (both are seen experimentally in ref 5), the radical orbital above the Ag Fermi level can be stabilized, picking up an electron to form a CC π- or CO σ-bonding orbital.

Conclusions

While not as active as O^- on oxide surfaces, oxygen atoms (formally O^{2-}) on a silver surface are clearly able to abstract hydrogen atoms from methyl groups. Empty metal surface orbitals at the Fermi level accept the electron that is released when O^{2-} becomes OH^-. It is expected that this reaction can occur on other metal surfaces with oxygen atoms chemisorbed on them. The activation energy should decrease for metals with higher electronegativities. The insertion of O(ads) into a methane CH bond to form CH_3OH(ads) is predicted to be possible in our calculations. In this case two electrons are promoted to the metal. It would be interesting to look for this potential carbene-like oxygen insertion reactivity over metal surfaces with oxygen overlayers.

Acknowledgment. This work was supported by a grant from the Gas Research Institute.

Registry No. CH_4, 74-82-8; *t*-BuO, 16331-65-0; H, 1333-74-0.

Carbonylation of Hydrocarbons via C–H Activation Catalyzed by $RhCl(CO)(PMe_3)_2$ under Irradiation

Toshiyasu Sakakura,[†] Touru Sodeyama,[†] Koushi Sasaki,[‡] Keisuke Wada,[‡] and Masato Tanaka*,[†]

Contribution from the National Chemical Laboratory for Industry, Higashi, Tsukuba, Ibaraki 305, Japan, and Research Center, Mitsubishi Kasei Corporation, 1000 Kamoshida-cho, Midori-ku, Yokohama 227, Japan.

Received May 25, 1989

Abstract: C–H bonds in hydrocarbons are carbonylated into aldehydes by reaction with carbon monoxide in the presence of $RhCl(CO)(PR_3)_2$ under irradiation. The reaction proceeds at an ambient temperature under an atmospheric pressure of CO. The catalytic activity of $RhCl(CO)(PR_3)_2$ decreases in the order $PMe_3 \approx$ 1,3,4-trimethylphospholane $\approx$ 1,3,4-trimethylphospholene $> P(CH_2O)_3CMe > PEt_3 \approx PBu_3 > P(i\text{-}Pr)_3 \approx PPh_3 \approx P(OMe)_3 >$ dppe. The thiocyanato complex exhibits a similar catalytic activity to the chloro complex. The use of other complexes of Co, Ir, and Ru resulted in much lower catalytic activities. In the carbonylation of benzene, benzophenone and benzyl alcohol are formed as byproducts. The yield of benzaldehyde reached 3.3% on the basis of benzene. Monosubstituted benzenes are converted mainly to meta-substituted benzaldehydes. In the reaction of *n*-alkanes, a terminal methyl group is selectively carbonylated to give a linear aldehyde. These regioselectivities are explainable in terms of thermodynamic stability of hydridoalkyl (or alkyl) intermediates. The linear aldehyde obtained from *n*-alkane undergoes a secondary photoreaction (Norrish Type II) to afford a terminal olefin and acetaldehyde. The catalytic activity, regioselectivity of the carbonylation, and the occurrence of Norrish Type II reaction are markedly affected by irradiation wavelength. $RhCl(PMe_3)_2$ formed via CO dissociation is proposed as a possible active species for the C–H activation.

Selective functionalization of hydrocarbons through C–H bond activation has been one of the most challenging problems facing organic chemists. Since some enzymes in nature are good catalysts for a wide range of transformations of alkanes, growing efforts have been made to synthesize artificial systems capable of C–H bond activation, in particular at the terminal methyl group. There are two different approaches to attain C–H bond activation. One is to mimic the structure of the active site of enzymes. So called "P-450 model systems" are examples of such approaches. However, the regioselectivity so far achieved has been poor even though sophisticated model systems like bulky porphyrins[1] have been devised. The other approach is to mimic only the function of enzymes by designing artificial reaction systems where the transformation mechanism may be completely different from enzymatic processes. A recent interesting example along this line is the zeolite-supported heterogeneous catalyst with which terminal selective oxidation of *n*-alkane was attempted.[2] However, the regioselectivity was also unsatisfactory. Another possibility belonging to the latter approach might be the renewed interest in the oxidative addition of alkane C–H bonds initiated by Bergman, Graham, and Jones.[3] In their systems, the primary C–H bond of terminal methyl groups was selectively cleaved while secondary C–H bonds remained intact.[3c,d] This selectivity is the reverse of that achieved by conventional functionalizations of alkanes with radicals or strong acids[4] and is not explainable by the order of bond strength. We have been investigating the application of this unique elemental step (oxidative addition of C–H bonds) to catalytic reactions, resulting in the recent development of the

---

[†] National Chemical Laboratory for Industry.

[‡] Mitsubishi Kasei Corporation.

(1) Cook, B. R.; Reinert, T. J.; Suslik, K. S. *J. Am. Chem. Soc.* **1986**, *108*, 7281–7286.

(2) Herron, N.; Tolman, C. A. *J. Am. Chem. Soc.* **1987**, *109*, 2837–2839.

(3) (a) Janowicz, A. H.; Bergman, R. G. *J. Am. Chem. Soc.* **1982**, *104*, 352–354. (b) Hoyano, J. K.; Graham, W. A. G. *J. Am. Chem. Soc.* **1982**, *104*, 3723–3725. (c) Jones, W. D.; Feher, F. J. *Organometallics* **1983**, *2*, 562–563. (d) Periana, R. A.; Bergman, R. G. *Organometallics* **1984**, *3*, 508–510.

(4) Pines, H. *The Chemistry of Catalytic Hydrocarbon Conversions*; Academic Press: New York, 1981. Pryor, W. A. *Free Radicals*; Mc-Graw Hill: New York, 1966.

0002-7863/90/1512-7221$02.50/0